Journal of Alloys and Compounds 509 (2011) 33–37

Contents lists available at ScienceDirect

Journal of Alloys and Compounds

journal homepage: www.elsevier.com/locate/jallcom

Reactive sintering study of a novel cemented carbide hard alloy $(W_{0.5}Al_{0.5})C_{0.5}$–Ni

Jianwei Liu[a,b], Xianfeng Ma[a,*], Huaguo Tang[a], Wei Zhao[a]

[a] State Key Laboratory of Rare Earth Resources Utilization, Changchun Institute of Applied Chemistry, Chinese Academy of Sciences, No. 5625 Renmin Street, Changchun 130022, Jilin, China
[b] Graduate School of Chinese Academy of Sciences, Beijing 100049, China

ARTICLE INFO

Article history:
Received 22 June 2010
Received in revised form 18 August 2010
Accepted 26 August 2010

Keywords:
Novel cemented carbide
Microstructure
Mechanical properties
Hard materials
WC

ABSTRACT

Cemented carbides hard alloy $(W_{0.5}Al_{0.5})C_{0.5}$–13.3 vol% Ni was successfully prepared by reactive sintering of carbon, nickel powder and $W_{0.5}Al_{0.5}$ alloy powder. The novel cemented carbide hard alloy has superior mechanical properties. The influence of sintering time and temperature on the microstructure, mechanical properties and density of the specimens are well described. Interestingly, both sintering time and temperature have amazing influence on the mechanical properties, density and microstructure of the specimen. During the reactive sintering process, Ni was the binder phase for sintering $(W_{0.5}Al_{0.5})C_{0.5}$–Ni cemented carbide, and it also accelerated the reaction rate of synthesizing $(W_{0.5}Al_{0.5})C_{0.5}$. The reactive sintering is a good method for preparing cemented carbide hard alloy $(W_{0.5}Al_{0.5})C_{0.5}$–Ni. Another phenomenon is that no $WNi/W_3Ni_3C/NiC_x$ type phases are found in the bulk specimens, although it was prepared by reactive sintering the carbon, nickel powder and $W_{0.5}Al_{0.5}$ alloy powder directly and the carbon vacancy reach to the astonished 50% value.

1. Introduction

Due to its exceptional hardness and superior bending strength, cemented carbide hard alloy $(W_{1-x}Al_x)C_y$ ($x = 0.1–0.86$, $y = 0.1–0.5$) is becoming the most important hard material for cutting tools and mining industry. $(W_{1-x}Al_x)C_y$ is a deduction solid solution of Al in WC, and it is found to crystallize in the hexagonal space group *P–6m2* (187), and has the WC-type structure [1,2]. In our previous work, we have synthesized a new compound $(W_{0.5}Al_{0.5})C_{0.5}$–Co by hot-pressing sintering cobalt and $(W_{0.5}Al_{0.5})C_{0.5}$ powders [3]. It has superior mechanical properties than WC-Co system. But to date, no one has used reactive sintering method to prepare $(W_{0.5}Al_{0.5})C_{0.5}$–Ni cemented carbide hard alloy directly by $W_{0.5}Al_{0.5}$/C/Ni powder. The main reason is that it is easy to form $WNi/W_3Ni_3C/NiC_x$ phases [4–6]. And among the perspective production methods of inter-metallic, reactive sintering has attracted a great interest. This method involves preparation of solid solution compounds directly from elemental or sub-compound constituents, typically in powder form [7,8].

Therefore, in order to get the well sintered specimen with good mechanical properties, we choose $(W_{0.5}Al_{0.5})C_{0.5}$–13.3 vol% Ni as a respective sample to investigate its sinter ability. Moreover, the microstructure, mechanical properties and density as the function of sintering time and temperature are well described, and the cell parameters of the sintered sample are also presented.

2. Experimental details

Elemental powders of nickel (58 μm, 99.6 wt%), carbon (<3.4 μm, 99% purity) and the alloy powders $W_{0.5}Al_{0.5}$ (<2 μm, 99% purity) prepared by mechanical alloying [9] were used as raw materials.

The $W_{0.5}Al_{0.5}$ powder, carbon powder and nickel mixture powders were pressed into a cuboids of 40 mm × 10 mm × 10 mm at a compaction pressure of 350 MPa. And then the specimens were sintered in a vacuum sintering furnace with the following cycle: (a) heated from room temperature to the sintering temperature with a heating rate of about 8 °C min^{-1} (c) kept at the sintering temperature for different time (30, 60, 90, 120 150 and 180 min, respectively), (d) cooled down from the sintering temperature to 1000 °C at about 13 °C min^{-1}, and then furnace cooled from 1000 °C to room temperature.

The specimens were investigated by X-ray diffraction (XRD), environmental scanning electron microscopy (ESEM) and energy dispersive analysis of X-ray (EDAX). The XRD analyses were performed on a D8 FOCUS X-ray diffractometer with Cu Kα radiation (λ = 1.5406 Å), operating at 40 Kv and 40 mA. The scanning speed was 8 min^{-1}. The microstructures of fracture surfaces were examined using environment scanning electron microscope (ESEM, HITACHI, S-4800) with a link EDAX system for local chemical composition analysis. The densities of the sintered specimens were

* Corresponding author. Tel.: +86 431 85262220; fax: +86 431 85698041.
E-mail address: xfma@ciac.jl.cn (X. Ma).

0925-8388/$ – see front matter © 2010 Elsevier B.V. All rights reserved.
doi:10.1016/j.jallcom.2010.08.118

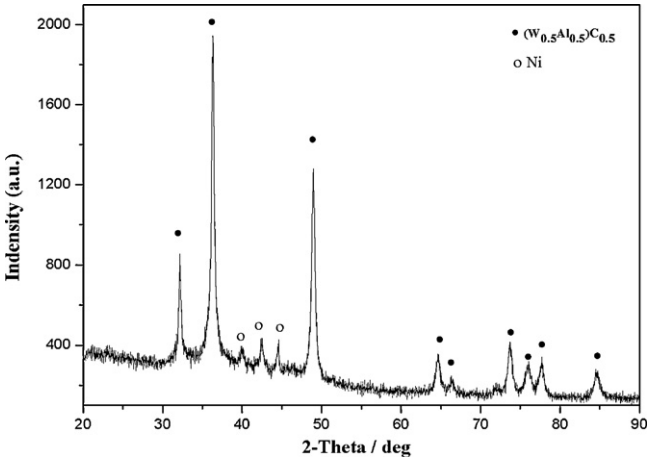

Fig. 1. The XRD patterns of $W_{0.5}Al_{0.5}C_{0.5}$–13.3 vol% Ni bulk alloy obtained by reactive sintering at 1410 °C for 150 min.

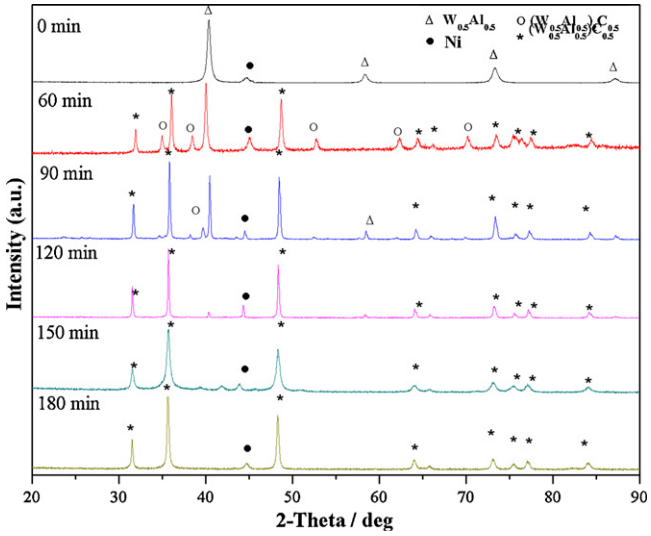

Fig. 2. The XRD patterns of $W_{0.5}Al_{0.5}C_{0.5}$–13.3 vol% Ni bulk alloy obtained by reactive sintering at 1410 °C for different time.

determined by the Archimedes water immersion method. Microhardnesses of the hard alloy bulk bodies were measured by the Vickers microhardness tester (FM-700, Japan) with a load of 300 gf and dwell time of 15 s. The transverse strengths were measured by three-point bending test. Bending tests were performed on an Instron model 1125 test machine at a crosshead speed of 2 mm/min; the distance of support of bending test was 30 mm, bending specimens (4 mm × 3 mm × 35 mm) were cut from the alloy bulk bodies. All the reported data were the average of at least three test results.

3. Results and discussion

3.1. X-ray diffraction and thermal stability

Fig. 1 shows the XRD patterns of $(W_{0.5}Al_{0.5})C_{0.5}$–13.3 vol% Ni bulk specimens sintered at 1410 °C after 150 min, as a respective sample of those sintered with various sintering condition. Sintered after 150 min, only the peaks of $(W_{0.5}Al_{0.5})C_{0.5}$ and nickel phases were observed. It can conclude that the cemented carbide $(W_{0.5}Al_{0.5})C_{0.5}$ had been synthesized completely by reactive sintering at 1410 °C after 150 min. There were also no peaks of structure of $WNi/W_3Ni_3C/NiC_x$ type phases. This means that nickel does not react with $W_{0.5}Al_{0.5}$ and/or carbon in the reactive sintering process.

Table 1 shows the EDX results of the $(W_{0.5}Al_{0.5})C_{0.5}$–13.3 vol% Ni. The ratio of W, Al, C is nearly 1:1:1. It can conclude that Al is still dissolved in the W. And seen from Fig. 1, there was no aluminum carbide (Al_4C_3) formation during the reactive sintering process, as evidenced by the absence of the Al_4C_3 peaks in the XRD patterns. This means that the alloy $W_{0.5}Al_{0.5}$ is still stable in the reactive sintering process. On the basis of XRD and EDX results, we can conclude that reactive sintering method is a suitable method to fabricate $(W_{0.5}Al_{0.5})C_{0.5}$–Ni cemented carbide hard alloy.

3.2. Impact of sintering time

Fig. 2 shows the XRD patterns of $(W_{0.5}Al_{0.5})C_{0.5}$–13.3 vol% Ni bulk specimens obtained by reactive sintering at 1410 °C for different time (0, 60, 90, 120, 150 and 180 min, respectively). Seen from the picture, at the beginning of the sintering process, $(W_{0.5}Al_{0.5})C_{0.5}$ and intermediate phase $(W_{0.5}Al_{0.5})_2C_{0.5}$ are formed under the force of high temperature. With the passage of time, $(W_{0.5}Al_{0.5})C_{0.5}$ increases and $(W_{0.5}Al_{0.5})_2C_{0.5}$ decreases step by step, eventually leading to the formation of $(W_{0.5}Al_{0.5})C_{0.5}$ with a carbon vacancy of about 50% completely after 120 min. The process is similar to the formation of $(W_{0.5}Al_{0.5})C_{0.5}$ by solid-state reaction [10]. From 120 to 150 min, the XRD patterns almost have no change. So it can be concluded that the fabrication of $(W_{0.5}Al_{0.5})C_{0.5}$–Ni by reactive sintering involved two stages: reaction stage (almost 0–120 min) and sintering stage (after 120 min). Consequently, to get well bulk hard alloy, the sintering time must be not <120 min.

Fig. 3 shows the SEM micrographs of fracture surface of $(W_{0.5}Al_{0.5})C_{0.5}$–13.3 vol% Ni sintered at 1410 °C for 60, 90, 120, 150 and 180 min, respectively. Seen from the picture, we can find that crystalline phase increases when the reaction time prolonged from 30 to 120 min. It is identical with the XRD result, the $W_{0.5}Al_{0.5}$ particles react with carbon particles completely after sintering for 120 min. And it also can be concluded that the sample nearly reach full density after sintering for 120 min for there is almost no pore in the specimen. When the sintering time went on to 180 min, grain size of the sample grows a little. Consequently, on the temperature of 1410 °C, the grain growth mainly takes place in the first 120 min (reaction stage).

Fig. 4 shows the Vickers microhardness and density of the simple sintered after 60, 90, 120, 150 and 180 min, respectively. The results reveal that, in the first 120 min, the hardness and density increase sharply with the prolonged sintering time. It is mainly because of the increase of the content of hard phase $(W_{0.5}Al_{0.5})C_{0.5}$. And the

Table 1
The results of EDX results of $(W_{0.5}Al_{0.5})C_{0.5}$–13.3 vol% Ni bulk specimens obtained by reactive sintering at 1410 °C for 150 min.

Element	Series	unn. C (wt.%)	norm. C (wt.%)	Atom. C (at.%)	Error (%)
Tungsten	L-series	70.44	70.31	27.13	0.3
Aluminum	K-series	11.26	11.06	27.32	0.2
Nickel	K-series	13.99	13.88	17.61	0.3
Carbon	K-series	5.68	4.75	27.94	1.2
Total		101.37	100	100	

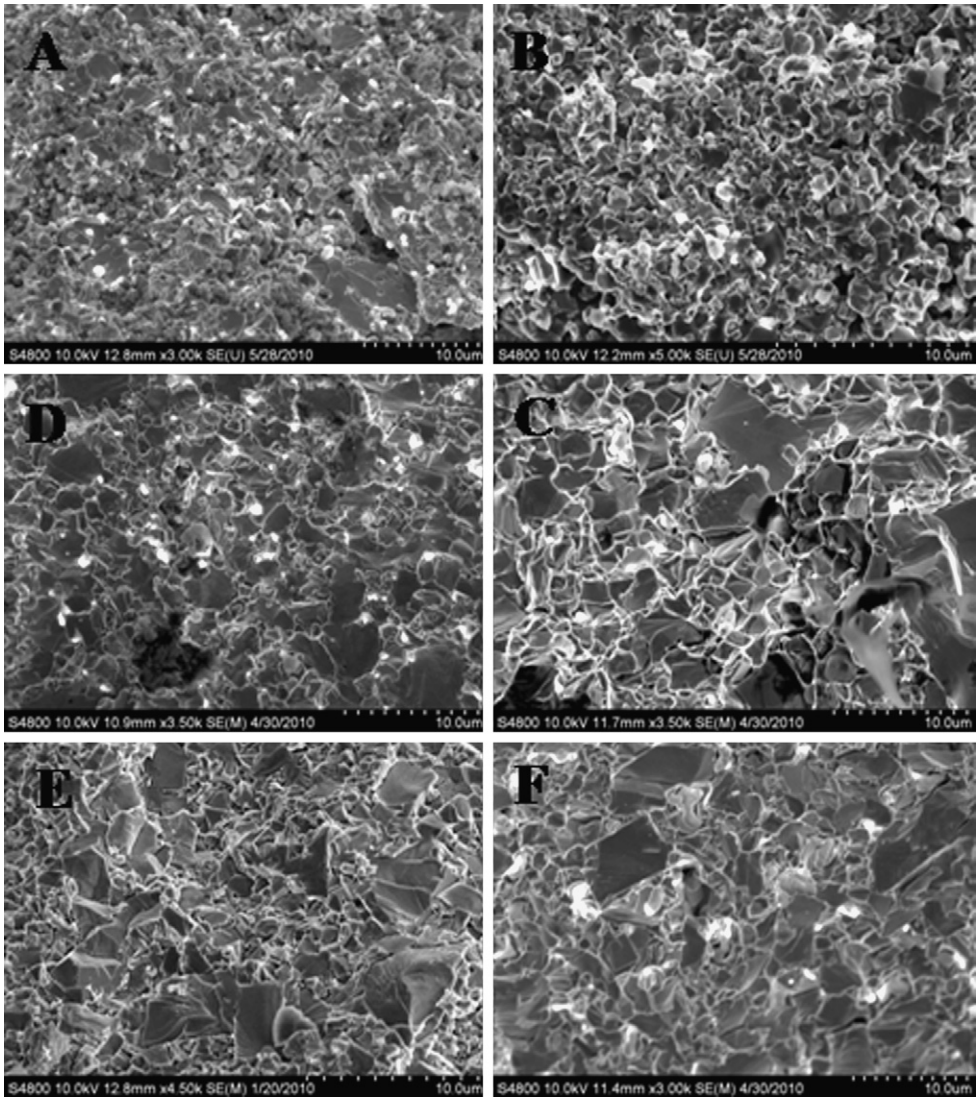

Fig. 3. The SEM micrograph of $(W_{0.5}Al_{0.5})C_{0.5}$–13.3 vol% Ni bulk specimen obtained by reactive sintering at 1410 °C for: (A) 30, (B) 60, (C) 90, (D) 120, (E) 150 and (F) 180 min.

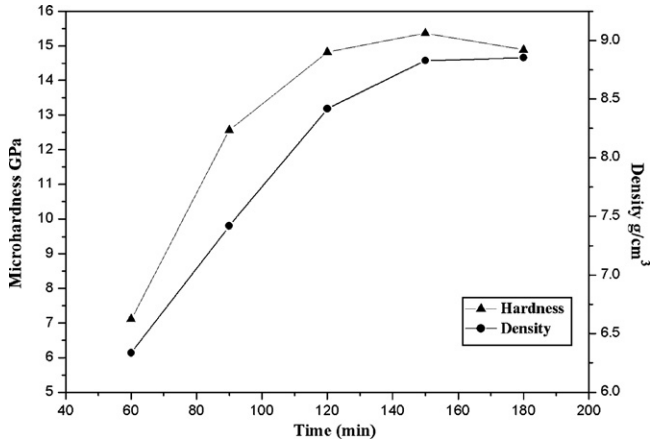

Fig. 4. The microhardness and density of $W_{0.5}Al_{0.5}C_{0.5}$–13.3 vol% Ni bulk specimens sintered at 1410 °C for different time.

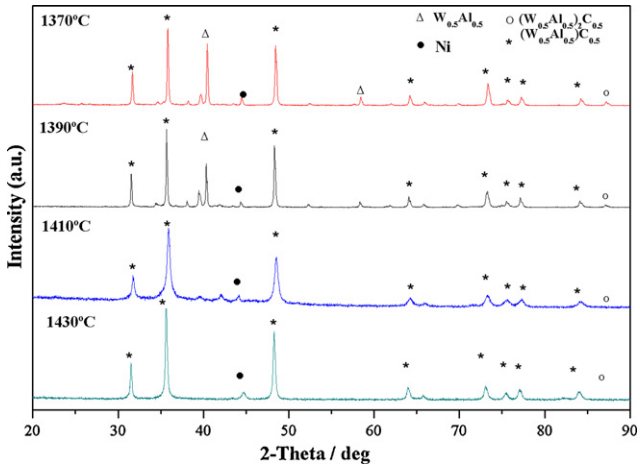

Fig. 5. The XRD patterns of $W_{0.5}Al_{0.5}C_{0.5}$–13.3 vol% Ni bulk alloy obtained by reactive sintering at different temperature after 150 min.

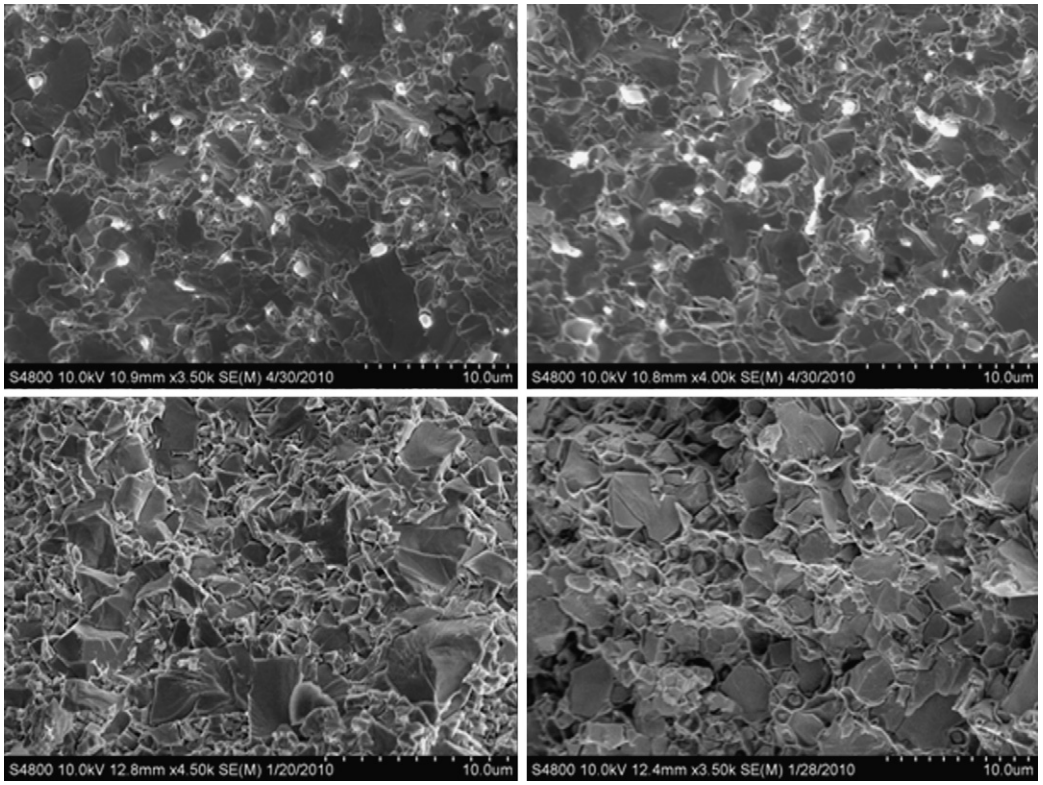

Fig. 6. The SEM micrograph of $(W_{0.5}Al_{0.5})C_{0.5}$–13.3 vol% Ni bulk specimen obtained by reactive sintering for 150 min at (A) 1370 °C, (B) 1390 °C, (C) 1410 °C and (D) 1430 °C.

decreased residual porosity doubtlessly contributes to the increase of the hardness and density too. And from 120 to 150 min, the hardness of the sample increases slightly with the prolonged sintering time. That is mostly because the density of the sample increases continuously during the sintering stage. Later on, as the sintering time continues to be prolonged, the density almost has not changed while the hardness becomes slightly decreasing (<2%). This slight decrease of hardness may due to the growth of particle size.

3.3. Impact of sintering temperature

Fig. 5 shows the XRD patterns of $(W_{0.5}Al_{0.5})C_{0.5}$–13.3 vol% Ni bulk specimens obtained by reactive sintering at different temperature after 150 min. It can be clearly seen that the reaction temperature has a remarkable influence on the formation of the $(W_{0.5}Al_{0.5})C_{0.5}$ in the reaction sintering stage. W_2C type peaks still can be seen in the XRD results of the specimens sintered at 1370 and 1390 °C for 150 min. We can conclude that with the increase of the reaction temperature, reaction rate of synthesizing $(W_{0.5}Al_{0.5})C_{0.5}$ continuously increases.

Fig. 6 shows the effect of sintering temperature on the morphology of the samples. It can be found that at 1370 °C, the grain size is almost 2 μm, but when the temperature arrives at 1430 °C, the grain size grows obviously and reaches 3–4 μm as shown. On the basis of these results, we can conclude that the temperature is one of key factors that affect the grain growth during the sintering process.

Fig. 7 shows the Vickers microhardnesses and bending strengths of the simple sintered at 1370, 1390, 1410 and 1430 °C, respectively. It can be clearly seen that with the increase of temperature from 1370 °C up to 1410 °C, the hardness increases remarkably to the maximum of 15.37 GPa. The bending strength also increases when the temperature up from 1370 to 1410 °C. But as the temperature reaches to 1430 °C, the bending strength of the sample decreases to 1913 MPa. This might be attributed to their difference

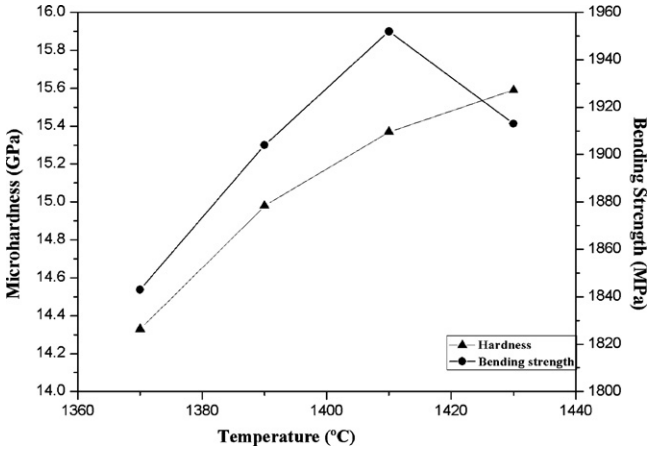

Fig. 7. The microhardness and bending strength of $W_{0.5}Al_{0.5}C_{0.5}$–Ni bulk specimens sintered at different temperature for 150 min.

of microstructure, the finer the grain size. In addition, when we further increase the temperature, the bending strength of the sintered sample continues to slightly decrease.

Based on the above results, we can conclude that the optimal condition for reactive sintering $(W_{0.5}Al_{0.5})C_{0.5}$–Ni is under the temperature 1410 °C for 150 min.

4. Conclusions

Reactive sintering of the hard alloy $(W_{0.5}Al_{0.5})C_{0.5}$–Ni has been varying the sintering temperature and time. The results show that sintering temperature and time are both important factors that influence the mechanical properties, density and microstructure. The most suitable sintering condition from our work is under the temperature 1410 °C for 150 min and the relative density reaches

98%. The resultant hardness is as high as 15.37 GPa, the resultant bending strength reaches 1952 MPa. It is interesting that no WNi/W_3Ni_3C/NiC_x type phases were formed during the sintering process, although it is prepared directly by reactive sintering carbon, nickel powder and $W_{0.5}Al_{0.5}$ alloy powder and the carbon vacancies get the value of 50%.

Considering its superior mechanical properties, lower density, and the simple producing technology, $(W_{0.5}Al_{0.5})C_{0.5}$–Ni hard alloys are expected to be new cemented carbides can replace the standard materials for cutting tools, wear parts, electrode materials, etc.

Acknowledgment

This work was supported by the National Natural Science Foundation of China with program: 20921002.

References

[1] J.M. Yan, X.F. Ma, W. Zhao, H.G. Tang, C.J. Zhu, Synthesis, crystal structure, and density of $(W_{1-x}Al_x)C$, J. Solid State Chem. 177 (2004) 2265–2270.
[2] H.G Tang, X.F. Ma, W. Zhao, X.W. Yan, J.M. Yan, Synthesis, reactive mechanism and thermal stability of $W_{1-x}Al_xC$ (x = 0.33, 0.5, 0.75, 0.86) nanocrystalline, Mater. Res. Bull. 39 (2004) 707–713.
[3] Z.H. Qiao, X.F. Ma, W. Zhao, H.G. Tang, B. Zhao, Nanostructured novel cemented hard alloy obtained by mechanical alloying and hot-pressing sintering and its applications, J. Alloy Compd. 462 (2008) 416–420.
[4] J.S.C. Jang, J.C. Fwu, L.J. Chang, G.J. Chen, C.T. Hsu, Study on the solid-phase sintering of the nano-structured heavy tungsten alloy powder, J. Alloy Compd. 434 (2007) 367–370.
[5] M. Bahgat, M.K. Paek, J.J. Pak, Reduction investigation of WO_3/NiO/Fe_2O_3 and synthesis of nanocrystalline ternary W–Ni–Fe alloy, J. Alloy Compd. 472 (2009) 314–318.
[6] M.R. Andrews, Production and characteristics of the carbides of tungsten, J. Phys. Chem.-Us 27 (1923) 270–283.
[7] P. Novak, A. Michalcova, M. Voderova, M. Sima, J. Serak, D. Vojtech, K. Wienerova, Effect of reactive sintering conditions on microstructure of Fe–Al–Si alloys, J. Alloy Compd. 493 (2010) 81–86.
[8] J.B. Fogagnolo, E.M.J.A. Pallone, D.R. Martin, C.S. Kiminami, C. Bolfarini, W.J. Botta, Processing of Al matrix composites reinforced with Al–Ni compounds and Al_2O_3 by reactive milling and reactive sintering, J. Alloy Compd. 471 (2009) 448–452.
[9] H.G. Tang, X.F. Ma, W. Zhao, X.W. Yan, R.J. Hong, Preparation of W–Al alloys by mechanical alloying, J. Alloy Compd. 347 (2002) 228–230.
[10] J.M. Yan, X.F. Ma, W. Zhao, H.G. Tang, C.J. Zhu, S.G. Cai, Crystal structure and carbon vacancy hardening of $(W_{0.5}Al_{0.5})C_{1-x}$ prepared by a solid-state reaction, Chem. Phys. Chem. 6 (2005) 2099–2103.